



## Heat-tolerant subtropical *Porites lutea* may be better adapted to future climate change than tropical one in the South China Sea

Wen Huang<sup>a,\*</sup>, Jinlian Chen<sup>a</sup>, Enguang Yang<sup>a</sup>, Linqing Meng<sup>a</sup>, Yi Feng<sup>a</sup>, Yinmin Chen<sup>a</sup>, Zhihua Huang<sup>a</sup>, Ronghua Tan<sup>a</sup>, Zunyong Xiao<sup>c</sup>, Yupeng Zhou<sup>c</sup>, Mingpei Xu<sup>c</sup>, Kefu Yu<sup>a,b,\*\*</sup>

<sup>a</sup> Guangxi Laboratory on the Study of Coral Reefs in the South China Sea, Coral Reef Research Center of China, School of Marine Sciences, Guangxi University, Nanning 530004, China

<sup>b</sup> Southern Marine Science and Engineering Guangdong Laboratory (Guangzhou), Guangzhou 511458, China

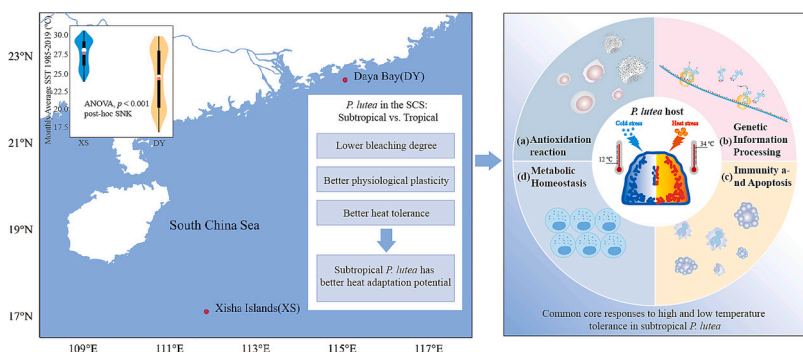
<sup>c</sup> School of Resources, Environment and Materials, Guangxi University, Nanning 530004, China

### HIGHLIGHTS

- The heat resistance of *Porites lutea* varies at different latitudes in the SCS.
- Subtropical *P. lutea* has a stronger heat tolerance.
- Better heat tolerance associated with a negative feedback transcription mechanism
- Subtropical *P. lutea* in the SCS may adapt to future climate change.

### GRAPHICAL ABSTRACT

***P. lutea* sample collection locations. (a) Violin plots of sampling locations and monthly mean sea temperature in the two regions. (b) Monthly mean and standard deviation of sea temperature at the sampling location. (c) Temperature design of the heat stress experiment.**



### ARTICLE INFO

Editor: Sergi Diez Salvador

#### Keywords:

*Porites lutea*  
Latitude  
Heat stress  
Heat resistance  
Climate change

### ABSTRACT

Coral reefs are degrading at an accelerating rate owing to climate change. Understanding the heat stress tolerance of corals is vital for their sustainability. However, this tolerance varies substantially geographically, and information regarding coral responses across latitudes is lacking. In this study, we conducted a high temperature (34 °C) stress experiment on *Porites lutea* from tropical Xisha Islands (XS) and subtropical Daya Bay (DY) in the South China Sea (SCS). We compared physiological levels, antioxidant activities, and transcriptome sequencing to explore heat tolerance mechanisms and adaptive potential. At 34 °C, both XS and DY corals experienced significant bleaching and the physiological/biochemical index decreased, with XS corals exhibiting greater changes than DY corals. Transcriptome analysis revealed that coral hosts respond to heat stress mainly by boosting metabolic activity. The subtle transcriptional responses of zooxanthellae C15 underscored the host's pivotal role in thermal stress responses. DY coral hosts showed lower bleaching, stronger physiological plasticity,

\* Corresponding author.

\*\* Correspondence to: K. Yu, Southern Marine Science and Engineering Guangdong Laboratory (Guangzhou), Guangzhou 511458, China.

E-mail addresses: [wenhuang@gxu.edu.cn](mailto:wenhuang@gxu.edu.cn) (W. Huang), [kefuyu@scsio.ac.cn](mailto:kefuyu@scsio.ac.cn) (K. Yu).

<https://doi.org/10.1016/j.scitotenv.2025.178381>

Received 9 July 2024; Received in revised form 28 November 2024; Accepted 2 January 2025

Available online 11 January 2025

0048-9697/© 2025 Elsevier B.V. All rights are reserved, including those for text and data mining, AI training, and similar technologies.

and higher temperature tolerance thresholds than XS, indicating superior heat tolerance. This superiority is linked to negative feedback transcriptional regulation strategies, including active environmental stress response and genetic information damage repair. The differences in thermal adaptability between tropical and subtropical *P. lutea* in the SCS may be attributed to their genetic differences and native habitat environments, suggesting that subtropical *P. lutea* may have the potential to adapt to future climate change. This study provides novel insights for predicting the fate of corals at different latitudes in terms of global warming and provides instructive guidance for coral reef ecological restoration.

## 1. Introduction

Climate change and anthropogenic factors have driven coral reef degradation (Hughes et al., 2003; Hughes et al., 2017). High sea surface temperatures (SST) owing to global warming have led to severe thermal bleaching events, posing a serious threat to coral reef survival (Ainsworth et al., 2016; Hughes et al., 2003). As climate warming persists, these bleaching events are expected to become more frequent and intense (Sully et al., 2019). Therefore, under current climate scenarios, corals must adapt in order to survive over the long term. However, the extent of their adaptability to thermal changes (Mumby and van Woesik, 2014) and the mechanisms by which naturally resilient corals might enhance their tolerance to climate change remains unclear (Langlais et al., 2017; Sully et al., 2019). Therefore, understanding these factors is crucial for assessing the future viability of coral ecosystems.

Temperature fluctuations of 1–2 °C above or below normal levels can prove fatal for narrowly temperate corals (Hoegh-Guldberg, 1999), although these thresholds vary across regions (Langlais et al., 2017; Sully et al., 2019). In addition, coral thermal tolerance thresholds are also related to factors such as coral holobionts genetic adaptation (Howells et al., 2016; Manzello et al., 2019), recent thermal history (Voolstra et al., 2020), latitude (Dixon et al., 2015), depth (Tavakoli-Kolour et al., 2023), and species (Marzoni et al., 2022). Recent fieldwork suggests that, in some locations, reef-building corals can tolerate heat stress at temperatures that exceed the global average (Masoudi and Asrari, 2023), particularly in habitats with thermal extremes (e.g., corals in the Persian–Arabian Gulf can tolerate water temperatures of 36 °C) (Coles and Riegl, 2013; D'Angelo et al., 2015), and thermal hyper-variability (e.g., corals in the American Samoan back reef tanks of Ofu Island at 35 °C) (Palumbi et al., 2014). However, these findings are mostly limited to specific regions, and widespread spatial heterogeneity exists in the thermal tolerance of corals (Langlais et al., 2017; Sully et al., 2019). Moreover, a clear understanding of the thermal tolerance responses and adaptive potential of corals across latitudinal temperature gradients is lacking.

Ecological studies have shown that coral species occupying a wide range of ecological niches span strong environmental temperature gradients and often vary phenotypically (Bruno and Edmunds, 1997; Rowan et al., 2021). Examples include Red Sea corals (Osman et al., 2017) and Australian Great Barrier Reef corals (Barfield et al., 2018). Further studies suggest that this phenotypic variation is related to local adaptation to the thermal regime of the host (Savary et al., 2021; Voolstra et al., 2021) as well as short-term physiological acclimation (Voolstra et al., 2021). Coral populations are undergoing strong regional selection for tolerance and exhibit significant individual genetic variability in response to rapid climate change (Barker, 2018; Quigley, 2023), offering potential for genetic rescue-assisted evolution to enhance their thermal resilience (Selmoni et al., 2024). Therefore, identifying temperature-tolerant coral populations at similar spatial scales is required to restore coral reef ecosystems.

South China Sea (SCS) coral reefs, with their large latitudinal spans and notable temperature gradients, provide a unique natural laboratory for exploring intra- and intercommunity coral responses to climate change (Yu, 2012). Agglomerated *Porites lutea* is considered a highly resistant coral species widely distributed in the Indo-Pacific reef zone in tropical and subtropical regions (Huang et al., 2015, 2012). *P. lutea* is an

ideal research species for studying various stress responses and coral physiology, and is a dominant species in SCS coral reefs (Li et al., 2013). Robbins et al. (2019) revealed the genome of *P. lutea*, including its symbiotic dinoflagellate *Cladocopium* C15 and associated microorganisms, providing a foundational resource for molecular studies. Preliminary studies on *P. lutea* in the SCS have been conducted. For example, Huang et al. (2018) reported high genetic diversity and low genetic differentiation levels in *P. lutea* populations from different geographic locations in the SCS. Luo et al. (2022) demonstrated a close correlation between genetic differentiation, genetic variation levels, and latitudinal SST. Additionally, Huang et al. (2022) used metatranscriptome sequencing methods to explore the differences in the cold tolerance of *P. lutea* at different latitudes in the SCS. However, regarding global warming, the heat resistance response of *P. lutea* at different latitudes in the SCS is not yet fully understood, and the underlying molecular mechanisms remain lacking.

In this study, we used physiological and metatranscriptome sequencing to explore the response and underlying adaptation mechanisms of *P. lutea* to thermal stress at different latitudes in the SCS. Additionally, we conducted association analyses by combining previous findings on cold stress and population genetics to explore understanding of the survival status and environmental stress adaptability of *P. lutea* to climate change. By shedding light on the adaptability of corals at diverse latitudes amid ongoing climate warming, this research offers instructive guidance for conserving and ecologically rehabilitating coral reefs.

## 2. Materials and methods

### 2.1. Sample collection and experimental design

*P. lutea* samples were collected from two latitudes in the South China Sea, namely the tropical Xisha XS North Reef (111°51'E, 17°06'N) and subtropical Daya Bay DY Sanmen Island (114°64'E, 22°27'N), with a latitudinal span of approximately 5° (see Fig. 1a for sampling point details). The 5 km daily mean SST data were obtained from NOAA's Coral Reef Watch (<http://coralreefwatch.noaa.gov>). The monthly mean SSTs at different sampling locations (Fig. 1b) were obtained from a previous study (Huang et al., 2022). Colonies were collected at approximately the same depth (~5 m) at each sampling location using a scuba diving device with a hammer and tongs. Colonies were sampled >5 m apart to avoid gene cloning. After sampling, the live coral samples were quickly transported to the 300 L aquarium tanks of the China Coral Reef Research Center of Guangxi University and temporarily restored at 26 °C. Five *P. lutea* were randomly selected from each sampling point for study. Three fragments (~16 cm<sup>2</sup> each) were removed from each coral using a small cutter to serve as three independent sampling points (26, 30, and 34 °C), i.e., each sampling point had five biological replicates, and one location had 15 fragments. All fragments were restored at 26 °C for 15 days before the formal experiment.

The heat stress experiment used three temperature treatments: 26 °C for the control group (optimal temperature for coral growth), 30 °C (normal temperature in summer) and 34 °C (extremely high temperature) for the experimental group, with consistent temperature intervals between the sampling points (Fig. 1c). Owing to resource limitations, only two tanks were used in this experiment, namely the control (26 °C treatment, 5 fragments × 2 locations = 10) and the experimental (30 °C

and 34 °C treatments, 5 fragments  $\times$  2 locations  $\times$  2 treatments = 20 tanks. To simulate marine environment warming, the experimental tank was heated by 1 °C every 24 h starting at 26 °C. After reaching 30 °C, the temperature was maintained for three days, and samples were taken. The temperature was then further increased and samples were taken after three days at 34 °C. The heat stress experiment cycle was 12 days. Simultaneously, the control tank was maintained at 26 °C for 12 days and samples were collected.

All aquariums were illuminated using metal halide (250 W) and four T5HO lamps to simulate natural light in a 12 h:12 h light-dark cycle. Preheated and filtered seawater (20 %) was replaced daily to maintain the following water conditions: salinity 34–35 ppt, carbonate hardness (dKH) 7.3–7.5,  $c(\text{Ca}^{2+})$  380–400 ppm, and  $c(\text{Mg}^{2+})$  1200–1300 ppm. The aquarium temperature was controlled using 600 W aquarium heating rods and chillers, and continuously monitored and recorded with a HOBO thermometer ( $\pm 0.1$  °C accuracy). The corals were not fed during the experiment. The experimental and control tanks were maintained under the same conditions, except for the temperature difference.

## 2.2. Sample handling and measurement

### 2.2.1. Phenotypic and physiological index determination

The coral samples were photographed and recorded daily using an underwater camera. The black-and-white tape was used as a reference background for image intensity calibration, and the degree of coral bleaching was analyzed using the computerized photo analysis software Image Pro Plus (version 6.0) (Chow et al., 2016; Huang et al., 2022). Specifically, the original photo was converted to an 8-bit grayscale image with a gray of 0 for pure black dots and a gray of 255 for pure white dots and then calibrated for color intensity using black and white reference points around the optical quadrant. After obtaining the actual intensity of the reference points, the intensity readings of 0 to 255 (8-bit) were reset, with the lowest intensity reading representing black being set to 0 and the highest intensity reading being set to 255 representing white. Finally, the gray value of the calibrated coral surface was measured, and the degree of bleaching of the entire coral surface was calculated using a defined black-and-white reference. In this study, the coral was considered “healthy” at 26 °C, and its bleaching degree was 0. The gray value at this time = K, and the gray values at other temperatures were defined as X. The formula was calculated as follows:

$$\text{Coral bleaching degree} = (X - K) / (255 - K) \times 100\%$$

The maximum quantum yield ( $F_v/F_m$ ) of *P. lutea* was measured daily using Diving-PAM (Heinz Walz GmbH, Effeltrich, Germany) fluorometer. To ensure adequate relaxation time for the corals,  $F_v/F_m$  was measured 30 min after the dark adaptation period, as this parameter closely approximates the maximum photochemical efficiency of photosystem II (PSII) (Bilger et al., 1995; Huang et al., 2022; Warner et al., 1999). During measurements, the fiber optic cable of fluorometer was maintained approximately 1 cm above the coral surface. To ensure the authenticity of  $F_v/F_m$  values, all measurements were performed randomly five times at different locations in the fragments.

Symbiodiniaceae density was determined as previously described (Chow et al., 2016; Qin et al., 2019), using a recirculating Waterpik filled with filtered seawater (0.45  $\mu\text{m}$ ) to rinse the coral surfaces, and quantifying the total volume of tissue homogenate using a measuring cylinder. Subsequently, 50 mL of homogenate was centrifuged (3000  $\times g$  for 10 min at 4 °C), the supernatant was removed, 20 mL of filtered seawater was centrifuged, and de-supernatant was added (repeated thrice) to quantify the cell density. The collected algae-containing cell pellets were fixed in 4 % formaldehyde solution and counted using a hemocytometer. Symbiodiniaceae density (cells  $\text{cm}^{-2}$ ) was calculated by normalizing the number of symbionts with respect to the surface area of stony corals derived from the aluminum foil method (Johannes et al., 1970).

The chlorophyll *a* content was determined using the absorbance method. Homogenate (15 mL) was placed in a sterile centrifuge tube and centrifuged at 4000  $\text{rmin}^{-1}$  for 5 min at 4 °C. The supernatant was removed, precipitate fixed with 10 mL 90 % acetone, and extracted at 4 °C in the absence of light for 24 h. The solution was then centrifuged and resuspended and the supernatant was subjected to optical density measurements at wavelengths of 630 nm, 647 nm, 664 nm, and 750 nm using a microplate reader (Varioskan LUX). The chlorophyll *a* content ( $\mu\text{g}/\text{mL}$ ) was calculated using the published method (Jeffrey and Humphrey, 1975). Finally, the chlorophyll *a* content per unit area of coral ( $\mu\text{g}/\text{cm}^2$ ) was obtained by converting the surface area of the coral.

### 2.2.2. Enzyme activity assay

The catalase (CAT), superoxide dismutase (SOD), peroxidase (POD), and glutathione (GSH) activities in the coral symbionts measured in this study were determined using commercial kits (Nanjing Jiancheng Bioengineering Institute, Nanjing, China) in strict accordance with the manufacturer's recommendations. We used a bicinchoninic acid (BCA) protein analysis kit (Shanghai Bioengineering Co., Ltd., Shanghai, China) to determine the concentration of total supernatant protein

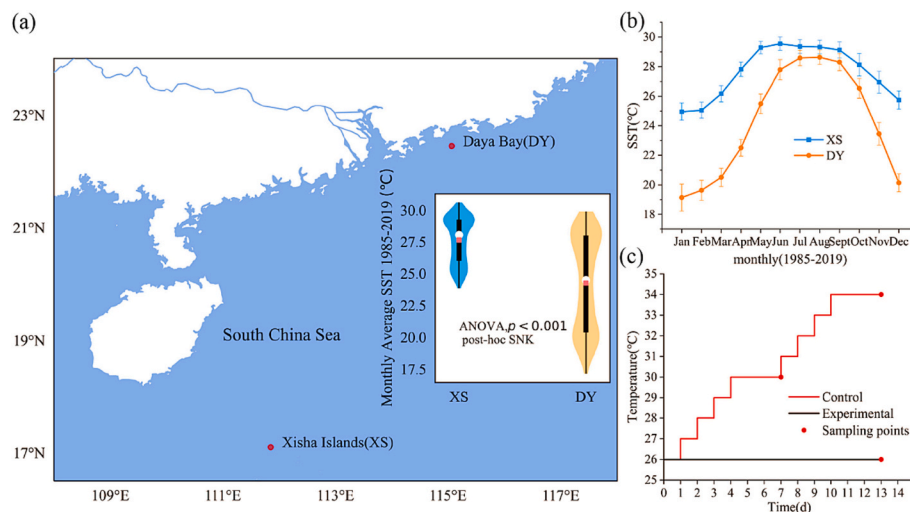


**Fig. 1.** *P. lutea* sample collection locations. (a) Violin plots of sampling locations and monthly mean sea temperature in the two regions. (b) Monthly mean and standard deviation of sea temperature at the sampling location. (c) Temperature design of the heat stress experiment.

according to the manufacturer's recommendations (Dodd and Drickamer, 2001). The enzyme activity in the sample supernatants was expressed as the ratio of total enzyme activity units to total protein (U/mg protein).

All data of physiological indices and enzyme activities were expressed as the mean  $\pm$  standard deviation (SD). Two-way analysis of variance (ANOVA) was used to analyze the main effects and interactions of the fixed factors (coral location and temperature). When main or interaction effects were significant ( $P \leq 0.05$ ), post hoc pairwise comparisons of variable means were conducted to determine if differences between coral locations in each temperature treatment were statistically significant (Lenth et al., 2019). Meanwhile, post-hoc multiple comparisons (Duncan's test) were used to determine the significance of data treated with different temperatures in the same coral location.

### 2.3. Symbiotic zooxanthellae identification

Genomic DNA was extracted from coral symbionts using the DNeasy Plant Mini Kit (QIAGEN, Hilden, Germany) according to the manufacturer's instructions. The ITS2 region of the symbiotic zooxanthellae rDNA was PCR amplified using ITS intfor2 (5'-GAATTGCAGA ACTCCGTG-3') (Lajeunesse and Trench, 2000) and ITS2-Reverse (5'-GGGATCCATA TGCTTAAGTT CAGCGGGT-3') (Coleman et al., 1994) primers (Chen et al., 2019). All qualified amplification products were mixed in equimolar amounts and subjected to nucleic acid sequencing using an Illumina MiSeq instrument in  $2 \times 300$  bp paired-end mode, according to the manufacturer's instructions. All sequencing was completed by Majorbio Biopharm Technology Co., Ltd. (Shanghai, China). The remainder of the analyses followed the method described by Chen et al. (2019). All the sequencing data were submitted to the NCBI for inclusion in the Biotechnology Information Sequence Read Archive database (accession no. PRJNA810338).

### 2.4. Transcriptome sequencing

#### 2.4.1. *P. lutea* RNA extraction

Following our established procedure, coral samples were carefully dissected, with a portion of coral tissue from each experimental sampling point placed individually into 2 mL sterile, enzyme-free centrifuge tube using RNA-removing enzyme-enzymatic forceps. Subsequently, the samples were rapidly frozen in liquid nitrogen for a minimum of 15 min, then transferred and stored in a  $-80^\circ\text{C}$  freezer for subsequent RNA extraction (Huang et al., 2022). Total RNA was extracted from each coral tissue sample using TRIzol (Life Technologies, USA), according to the manufacturer's instructions and product datasheet. RNA was purified using the MicroElute<sup>®</sup> RNA Clean Up Kit (Omega Biotech, Guangzhou, China) to remove contaminants, such as proteins, pigments, and polysaccharides, from the mixtures. The total RNA purity and concentration were measured using a NanoDrop 2000 UV-vis spectrophotometer (Thermo Fisher Scientific, Wilmington, VA, USA) (Desjardins and Conklin, 2010). RNA integrity was measured using the Agilent Bioanalyzer 2100 system (Agilent Technologies, Santa Clara, CA, USA).

Total RNA quality was assessed using 1 % agarose gel electrophoresis, and high-quality nucleic acid solutions were stored at  $-80^\circ\text{C}$  to prevent degradation from repeated freezing and thawing cycles.

#### 2.4.2. RNA-Seq analysis

RNA sequencing was performed using the Illumina Truseq<sup>™</sup> RNA Sample Prep Kit, and 12 cDNA libraries were constructed from tissue samples that met the requirements for library construction (total RNA  $> 1 \mu\text{g}$ , concentration  $> 35 \text{ ng}/\mu\text{L}$ , OD260/280  $> 1.8$ , OD260/230  $> 1.0$ ). A total of 12 cDNA libraries were constructed. Briefly, mRNA was enriched using magnetic beads with oligo (dT) for A-T base pairing with the poly A tails at their 3' ends. A fragmentation buffer was added to fragment the mRNA, and small fragments of approximately 300 bp were

separated via magnetic bead screening. Subsequently, using a reverse transcriptase, six-base random primers (random hexamers) and mRNA templates were reverse-transcribed to form a double-stranded structure with stable sticky ends. The paired-end RNA-seq library was sequenced using the Illumina NovaSeq 6000 platform ( $2 \times 150$  bp read length) by forming adaptor junctions and performing cDNA target fragment screening, amplification, and quantification. All the sequencing data were submitted to the NCBI for inclusion into the Biotechnology Information Sequence Read Archive database (accession no. PRJNA994659).

#### 2.4.3. Bioinformatics analysis

To ensure the accuracy of subsequent bioinformatics analysis, we removed the adapter sequences and incorrectly self-connected reads in the reads and trimmed the low-quality (quality value  $< 30$ ) bases at the end (3' end) of the sequence. Reads with an N-ratio of  $> 10\%$  were removed, and finally, the adapter and sequences with a length of  $< 50$  bp after quality trimming were discarded to obtain clean reads. The clean reads of each sample were then aligned to the *P. lutea* host and *Cladocopium* C15 reference genomes (Robbins et al., 2019) (<http://plutreefgenomics.org/>) using TopHat2 (Version 2.1.0) (Kim et al., 2013). Reads that matched the coral host genes were not further aligned to *Cladocopium* C15. BLAST alignment was performed using six databases: Non-redundant (NR), Swiss-prot, Pfam, Clusters of Orthologous Groups (COG), Gene Ontology (GO) and the Kyoto Encyclopedia of Genes and Genomes (KEGG). Successfully matched genes were annotated and the number of reads was mapped to each gene and counted using RMSE (Version 1.3.3) (Li and Dewey, 2011). Finally, gene expression levels were normalized using the transcripts per million (TPM) method. The normalized expressions of all 12 samples were hierarchically clustered using Spearman correlation, and the obtained numerical matrix was visually displayed using a Heatmap diagram. Differential expression analysis was performed using DESeq2 (Version 1.24.0) (Love et al., 2014), and genes with  $|\log_2(\text{Fold Change})| \geq 1$  and  $P_{\text{adjust}} < 0.05$  were classified as differentially expressed genes (DEGs). Genes with important functions were searched in the annotations of the DEG sets, and the expression changes were visualized. To study the biological functions of DEG functions, we used the KEGG database to enrich and analyze the various metabolic pathways. We evaluated the degree of enrichment of KEGG based on the rich factor, corrected  $P_{\text{adjust}}$ , and number of genes. When  $P_{\text{adjust}} < 0.05$ , the pathway was considered significantly enriched. To visualize the protein interaction network of the DEGs, we used String (version 11.5) and the homologous species, *Pocillopora damicornis*. The results were imported into Cytoscape (version 3.9.1) to map some of the gene networks using the top integrated values, and the Maximal Clique Centrality (MCC) algorithm in the software's built-in Cytohubba plugin was used to identify the top 10 hub genes of corals responding to high-temperature stress (Jeong et al., 2001). Because of the limited number of DEGs in zooxanthellae, we conducted expression change analysis for the entire gene set using Gene Set Enrichment Analysis (GSEA) to overcome the limitations of DEGs enrichment analysis.

## 3. Results

### 3.1. Physiological and biochemical indicator analysis of *P. lutea* under heat stress

#### 3.1.1. Phenotypic and physiological indicators

The differences in coral thermal bleaching phenotypes are related to heat resistance, thus the phenotypic variation plot showed that DY *P. lutea* had better heat resistance than XS (Fig. S1). In addition, consistent with the phenotypic changes, DY *P. lutea* had a lower bleaching degree and higher retention of maximum light quantum yield (*Fv/Fm*) than XS. In this high temperature stress experiment, the bleaching degree and *Fv/Fm* were significantly affected by coral geographical location, temperature, and location  $\times$  temperature (two-way ANOVA,  $P \leq 0.001$ ) (Fig. 2a, b). The severity of coral bleaching



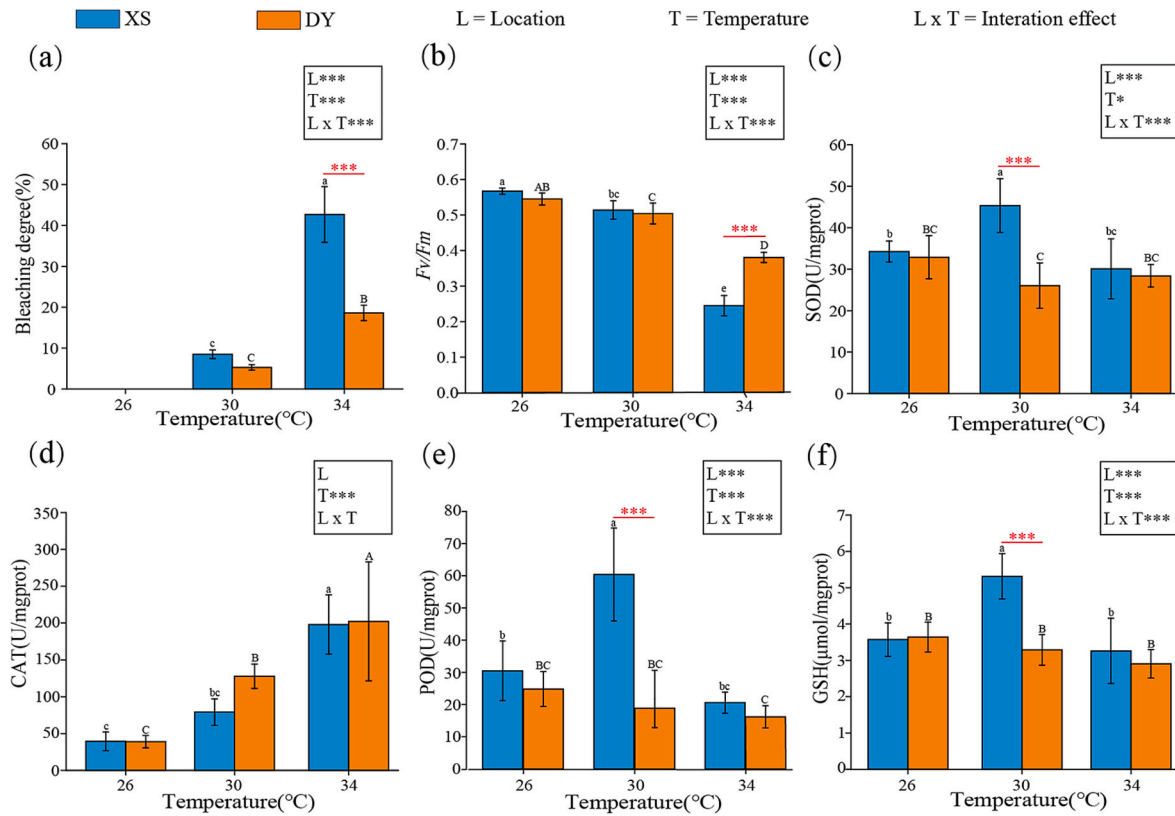


**Fig. 2.** Physiological and enzyme activity changes of coral samples. (a) bleaching degree. (b)  $F_v/F_m$ . (c) Superoxide dismutase, SOD. (d) catalase, CAT. (e) peroxidase, POD. (f) glutathione, GSH. Error bars represent SD of the mean obtained using multiple replicates. Error bars represent the standard deviation of the mean (SD,  $n = 5$ ) obtained using multiple replicates. Two-way ANOVA testing of coral location, temperature, and their interaction was framed ( $*P \leq 0.05$ ,  $**P \leq 0.01$ ,  $***P \leq 0.001$ ). Different lowercase or uppercase letters indicate that the parameters were significantly different between the temperature treatments (Duncan's test,  $P < 0.05$ ), respectively. Red asterisks indicate significant differences between two coral geographic locations at a given temperature ( $*P \leq 0.05$ ,  $**P \leq 0.01$ ,  $***P \leq 0.001$ ).

increased with increasing temperature (Fig. 2a). At 34 °C, the bleaching degree of corals at the two latitudes differed significantly with XS *P. lutea* being significantly more bleached than DY corals (pairwise test,  $P \leq 0.001$ ). In contrast,  $F_v/F_m$  decreased with increasing temperature, only decreasing significantly at 34 °C (Duncan's test,  $P > 0.05$ ) and differing significantly between the two latitude corals (paired test,  $P \leq 0.05$ ), indicating its significantly higher  $F_v/F_m$  in DY *P. lutea* than that in XS *P. lutea*.

### 3.1.2. Enzyme activity biochemical indicators

Two-way ANOVA results showed that SOD, CAT, GSH, and POD enzyme activities were significantly affected by temperature ( $P \leq 0.05$ ). Except for CAT, other enzyme activities were significantly affected by coral location and coral location  $\times$  temperature ( $P \leq 0.001$ ) (Fig. 2c–f).

Throughout the temperature-raising experiment, the levels of SOD, POD, and GSH in XS *P. lutea* initially increased and then decreased significantly ( $P < 0.05$ ). Among the antioxidants of DY *P. lutea*, SOD, POD and GSH all decreased slightly, but the changes were not significant ( $P > 0.05$ ). CAT activity was significantly increased in corals in both locations ( $P < 0.05$ ), and the CAT activity of DY *P. lutea* was higher than that of XS *P. lutea*, although not significantly ( $P \geq 0.05$ ) at each temperature. In corals from both latitudes, all enzyme activities, except that of CAT, differed significantly only at 30 °C, and the level of enzyme activity was significantly higher in XS *P. lutea*. In addition, at 34 °C, except for the CAT activity of the two groups of corals which was higher than that at 26 °C, the other antioxidant enzyme activities were lower than those at 26 °C, although not significantly ( $P > 0.05$ ).

### 3.2. RNA sequencing data and alignment rate

Twelve cDNA libraries were constructed, comprising samples from *P. lutea* hosts in XS and DY at 26 °C (C\_XS, C\_DY) and 34 °C (H\_XS, H\_DY). Transcriptome sequencing analysis of 12 coral host samples was completed, and a total of 80.42 Gb of clean data was obtained. The clean data of each sample reached >5.53 Gb, the Q30 base percentage was >93.86 %, and the GC content was between 42.11 and 46.44 %. The clean reads of each sample were aligned with the specified reference genome, with alignment rates between 40.08 and 69.72 %. In addition, transcriptome sequencing of the symbiotic zooxanthellae C15 obtained 30.89 Gb of clean data. Clean data for each sample exceeded 1.32 GB, with a Q30 base percentage exceeding 92.82 % and GC content ranging between 41.42 and 50.69 %. The alignment rate ranged from 0.63 and 34.45 %. The sequence information is provided in Table S1.

### 3.3. *P. lutea* host heat stress response

#### 3.3.1. Host gene expression analysis

In the sample correlation analysis, most of the *P. lutea* samples were clearly clustered into the control group at 26 °C and the high-temperature group at 34 °C (Fig. 3a). However, the XS3 sample deviated somewhat, and considering the slight differences between coral individuals, we retained all samples for subsequent analysis. At 34 °C, the expression level of the caspase-3 gene in coral hosts increased significantly, with the expression level in DY hosts being the highest. The expression levels of SOD-related functional genes at both latitudes increased slightly, whereas those of CAT- and GSH-related functional genes decreased; the decrease in expression in XS corals was lower than

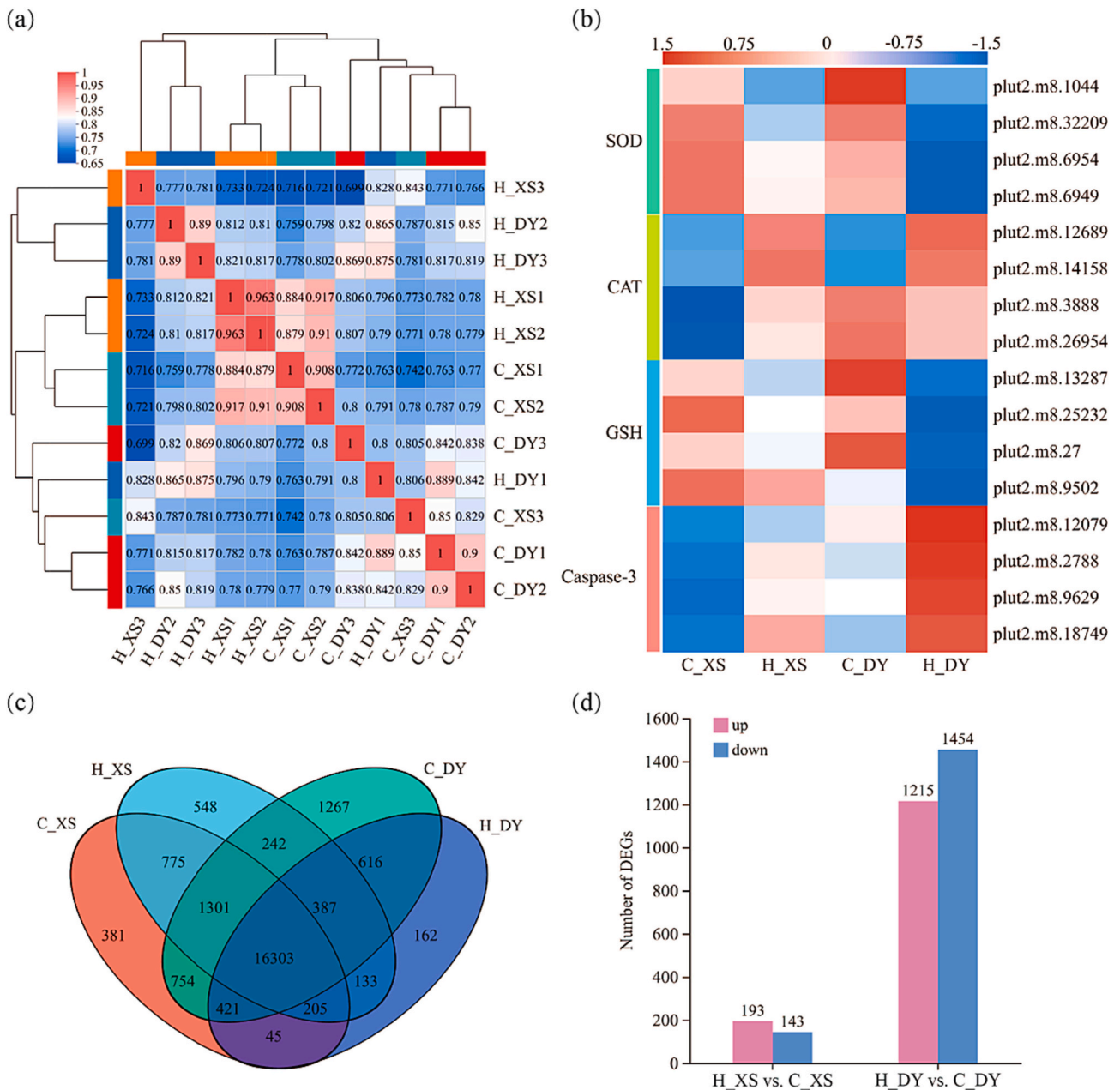


**Fig. 3.** Correlation between host genes and samples. (a) Heatmap showing changes in expression levels of functional genes during high-temperature stress. (b) Sample correlation clustering heat map (the numbers in the rectangles represent the correlation coefficients between samples). (c) Venn diagram of sequencing samples. (d) Number of DEGs in hosts (C: 26°C, H: 34°C).

that in DY corals (Fig. 3b). The number of common unigenes in all samples sequenced from *P. lutea* hosts (XS and DY) was 16,303. At 26 °C, the number of genes specific to XS and DY was 381 and 1267, respectively. At 34 °C, the number of genes unique to XS and DY was 548 and 162, respectively, indicating large differences in gene expression between XS and DY coral hosts (Fig. 3c).

### 3.3.2. Differential expression and enrichment analysis

The screening criteria were set as fold change  $\geq 2$  and false discovery rate value  $\leq 0.05$ , and differential expression analysis was performed on H\_XS vs. C\_XS and H\_DY vs. C\_DY. The results revealed 336 DEGs in XS *P. lutea* hosts at 34 °C compared to 26 °C, comprising 193 upregulated genes and 143 downregulated genes. A total of 2669 DEGs were identified in the DY coral host, of which 1215 were upregulated and 1454 were downregulated (Fig. 3d). The number of DEGs in the relatively

high-latitude DY coral hosts under heat stress was significantly higher than that in the XS coral hosts. Among the DEGs between the two groups of corals, 113 genes were upregulated (Hot\_two up) and 90 genes were downregulated (Hot\_two down) of the DEGs, 127 were XS-specific (Hot\_XS diff) and 2460 were DY-specific (Hot\_DY diff). KEGG enrichment analysis was performed for each of these gene sets, and the results are displayed in terms of the top 20 KEGG pathways (Fig. 4a–d).

KEGG enrichment analysis showed that compared with the control group (26 °C), the common upregulated DEGs of the two groups of coral hosts were significantly enriched in pathways related to metabolism, immune system, information processing, and disease infection. These pathways included Herpes simplex virus 1 infection, RIG-I-like receptor signaling pathway, cytosolic DNA-sensing pathway, shigellosis, influenza A, measles, glyoxylate and dicarboxylate metabolism, retinol metabolism, *Vibrio cholerae* infection, pathogenic *Escherichia coli*

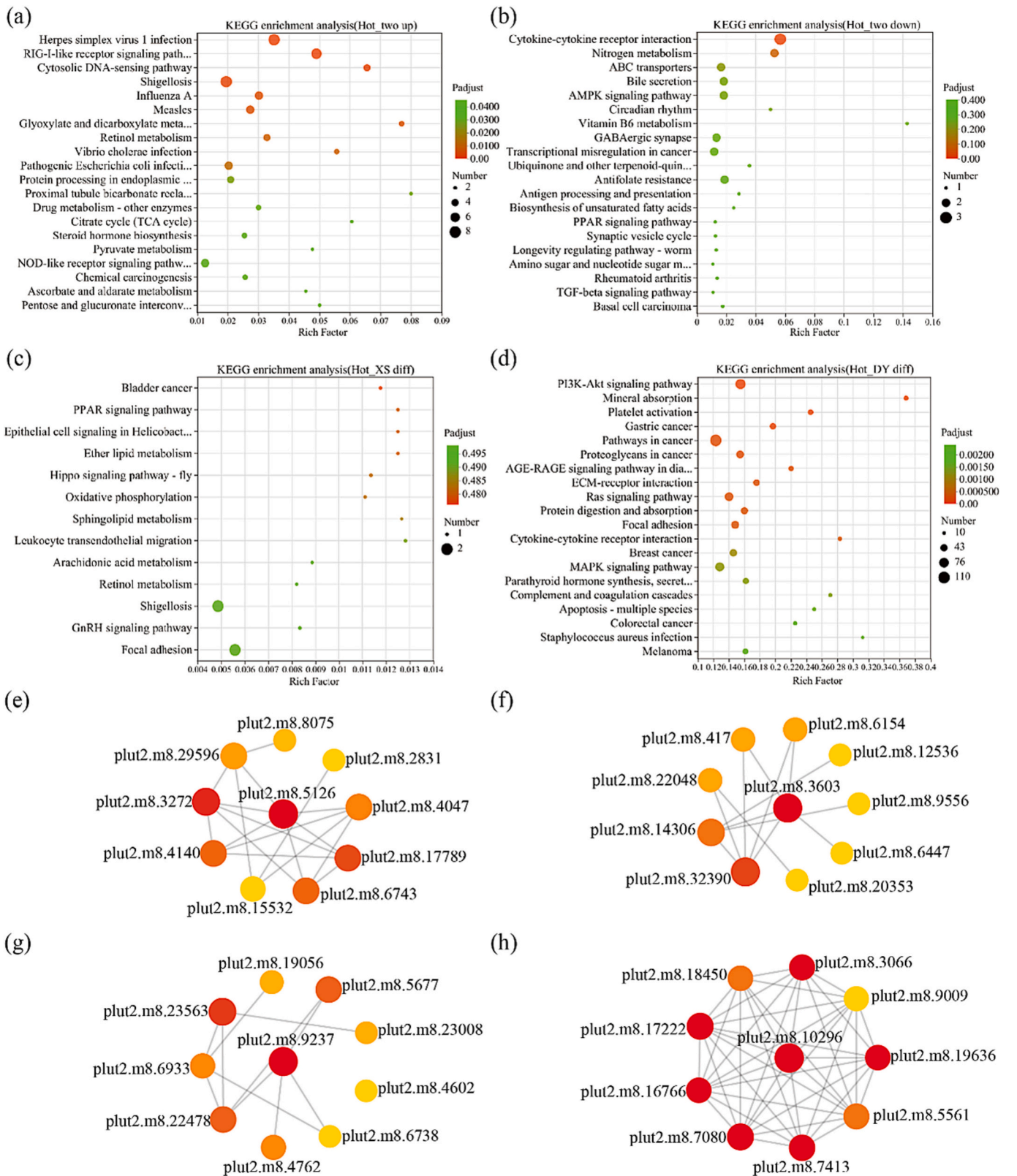


**Fig. 4.** KEGG pathway enrichment analysis and PPI network modules of host DEGs. KEGG enrichment analysis analyzed (a) significantly upregulated genes and (b) significantly downregulated genes in *P. lutea* samples from two regions. (c) XS-specific DEGs. (d) DY-specific DEGs. PPI network modules of (e) Hot\_two up; (f) Hot\_two down; (g) Hot\_XS diff; (h) Hot\_DY diff. Node color represents MCC score (The redder the color, the higher the score).



infection, protein processing in endoplasmic reticulum, proximal tubule bicarbonate reclamation, drug metabolism - other enzyme, TCA cycle, steroid hormone biosynthesis, pyruvate metabolism, NOD-like receptor signaling pathway, chemical carcinogenesis, ascorbate and aldarate metabolism, and pentose and glucuronate interconversions ( $P_{\text{adjust}} < 0.05$ ) (Fig. 4a). The common downregulated DEGs were only significantly enriched in the cytokine–cytokine receptor interaction pathway during environmental information processing ( $P_{\text{adjust}} < 0.05$ ) (Fig. 4b). Notably, XS-specific DEGs were not significantly enriched in any metabolic pathway ( $P_{\text{adjust}} > 0.05$ ) (Fig. 4c). However, DY-specific DEGs were significantly enriched in metabolic pathways related to environmental information processing, organic systems, and cellular processes. These pathways included the PI3K-Akt signaling pathway, mineral absorption, platelet activation, ECM-receptor interaction, Ras signaling pathway, protein digestion and absorption, focal adhesion, cytokine–cytokine receptor interaction, MAPK signaling pathway, arathyroid hormone synthesis, secretion and action, complement and coagulation cascades, and apoptosis-multiple species ( $P_{\text{adjust}} < 0.05$ ) (Fig. 4d).

### 3.3.3. DEGs protein–protein interaction (PPI) network module construction and hub gene screening

The XS and DY common DEGs, as well as the Hot\_XS diff and Hot\_DY diff gene set nodes, were ranked using the MCC score of the CytoHubba plugin. The top 10 genes with the highest scores were selected as hub genes for the PPI network module (Fig. 4e–h). We predicted that these hub genes have important biological relevance in the coral hosts to heat stress.

The top 10 hub genes in each of the four PPI network modules were analyzed for KEGG functional enrichment. Module (e) exhibited significant enrichment in pathways related to cellular energy metabolism, such as the citrate cycle (TCA cycle), pyruvate metabolism, proximal tubule bicarbonate reclamation, and longevity-regulating pathway-multiple species ( $P_{\text{adjust}} < 0.05$ ). Notably, heat shock protein genes (HSP) expression was upregulated in this pathway. Module (f) was significantly enriched in cytokine–cytokine receptor interactions, AMPK signaling pathway, and vitamin B6 metabolism ( $P_{\text{adjust}} < 0.05$ ). Module (g) was enriched in the chemical carcinogenesis and bile secretion pathways, albeit not significantly ( $P_{\text{adjust}} > 0.05$ ). Finally, module (h) was significantly enriched in the cell cycle ( $P_{\text{adjust}} < 0.05$ ), with upregulation of serine/threonine protein kinase genes CHK1,2, and cell division control protein genes CDC6 and CDC45.

## 3.4. Response of *P. lutea* algal symbionts to heat stress

### 3.4.1. Composition of symbiotic zooxanthellae in *P. lutea*

The dominant genus of symbiotic zooxanthellae across all coral samples was *Cladocopium*, and the dominant species was subclade C15 (Fig. S2a). Therefore, the community structure of symbiotic zooxanthellae in *P. lutea* at the two latitudes in this study was similar in composition and relative abundance, all dominated by the C15 subclade.

### 3.4.2. Analysis of gene expression and enrichment of algal symbiont C15

Consistent with the host analysis criteria, C15 zooxanthellae symbiotic with corals in XS and DY were analyzed. The results showed that C15 contained 11,934 common unigenes at different temperatures. At 26 °C, DY coral C15-specific unigenes outnumbered XS coral-specific unigenes, at 687 and 350, respectively (Fig. S2b). At 34 °C, XS coral-specific unigenes decreased to 107, while DY coral-specific unigenes slightly decreased to 149. Notably, the number of DEGs in C15 under high-temperature stress was minimal, while XS exhibited a total of 20 DEGs, including 11 upregulated and 9 downregulated genes (Fig. S2c). Nine DEGs were identified in the DY group, including seven upregulated and two downregulated genes. All possible pathways of XS and DY C15 were enriched using GSEA (Table S2). GSEA analysis showed that genes enriched for protein output were significantly downregulated in the XS and DY C15 groups compared with those in the control group.

Additionally, XS C15 significantly downregulated genes expression related to RNA polymerase, whereas DY C15 significantly downregulated genes expression related to proteasomes and spliceosomes.

## 4. Discussion

### 4.1. Response of *P. lutea* population to high-temperature stress in the SCS

During the heat stress process, the bleaching degree of the two groups of corals increased significantly with the change in temperature, and the density of zooxanthellae, *Fv/Fm*, and chlorophyll *a* content gradually decreased. These results suggest that rising temperatures can lead to coral bleaching, photodamage to photosynthetic system II, and disruption of the symbiotic relationship between the host and zooxanthellae (Evensen et al., 2021; Hazraty-Kari et al., 2023, 2024). Heat stress triggers the antioxidant mechanisms of corals and increases ROS levels in corals (DeSalvo et al., 2008). However, the coral–algae symbiosis can also effectively remove ROS via antioxidant systems, including POD, GSH, SOD and CAT (Anithajothi et al., 2014; Pei et al., 2022). Changes in the activity levels of these antioxidant enzymes and their genes expression, as well as the significant upregulation of the caspase-3 gene associated with cellular immune apoptosis, indicated that the corals have oxidative stress and apoptosis responses (Figs. 2, 3b).

Transcriptome sequencing results showed that high-temperature stress mainly activated pathways related to cell metabolism and apoptosis, inhibiting the expression of cytokine genes related to immune signaling (Fig. 4a, b). High-energy metabolic demands may suggest that the coral host is energy-limited and responds to cellular demands for energy balance by enhancing metabolism (Anthony et al., 2009). However, the KEGG enrichment analysis results of the DEGs upregulated by both were also significantly enriched in disease pathways related to viral or bacterial infections, indicating that extreme temperatures can significantly increase the risk of coral disease (Yu et al., 2023). In addition, the gene expression profile of zooxanthellae C15 was similar to that of *P. lutea* under low-temperature stress at different latitudes (Huang et al., 2022) with few significant DEGs in both groups (Fig. 5c). The GSEA of symbiotic zooxanthellae C15 showed that both XS and DY C15 significantly downregulated protein export-related genes at high temperatures. Protein export may be related to the activity of antioxidant-related proteins in symbiotic algae (Anithajothi et al., 2014; Buerger et al., 2020). The consistent downregulation of protein export-related genes alongside the substantial decrease in zooxanthellae density suggests that the high temperature of 34 °C may have damaged the organelles responsible for secreting antioxidants, leading to a significant loss of zooxanthellae, underscoring the decline in antioxidant enzyme content (Fig. 3f–i). In summary, the thermal tolerance of *P. lutea* mainly depends on the host itself (Huang et al., 2024; Yu et al., 2023). Furthermore, high-energy metabolism and antioxidant capacity are strategies for corals to avoid high-temperature threats and reduce oxidative damage.

### 4.2. Differences in heat tolerance between tropical XS and subtropical DY *P. lutea* in the SCS

Following exposure to heat stress at 34 °C, tropical *P. lutea* exhibited more severe bleaching than subtropical *P. lutea* and displayed a poorer physiological state characterized by lower zooxanthellae density, chlorophyll *a* content, and *Fv/Fm*. Therefore, we speculated that subtropical *P. lutea* is more heat-tolerant than tropical *P. lutea*. Notably, poor physiological status does not necessarily imply that XS *P. lutea* is completely incapable of regulating heat stress. We observed that during the entire heat stress process, the antioxidant enzyme activities of XS *P. lutea* changed significantly compared with DY coral, and the enzyme activity level was slightly higher at 34 °C. This finding suggested that tropical XS corals have a stronger antioxidant response to heat stress



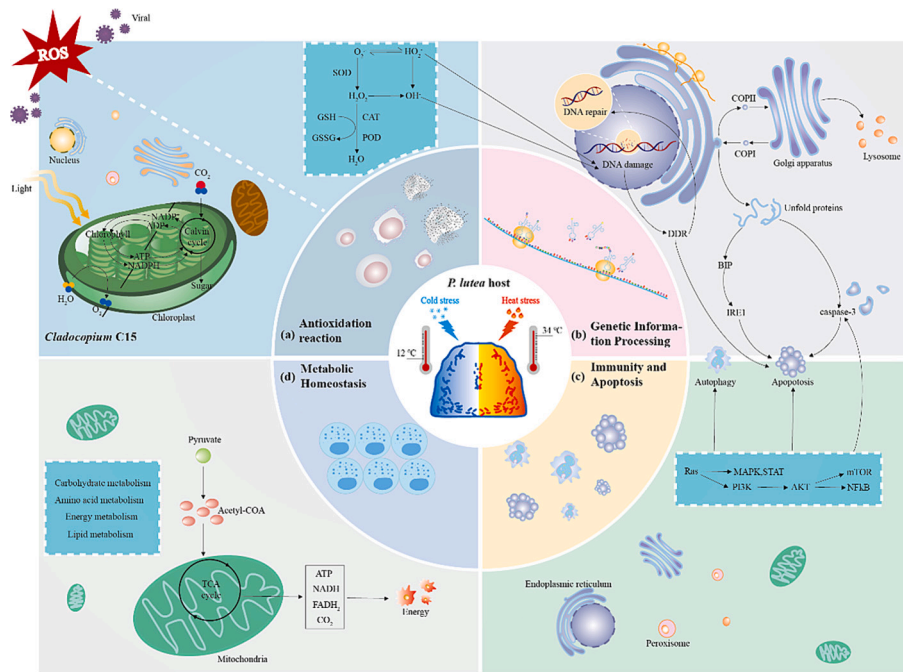


**Fig. 5.** Common core stress responses of *P. lutea* that are more tolerant to temperature stress. Genes and pathways related to (a) antioxidation reaction, (b) genetic information processing, (c) immunity and apoptosis, and (d) metabolic homeostasis are shown.

than subtropical DY corals, probably because XS *P. lutea* survives for a long period in waters with higher SSTs and can respond rapidly to heat stress by regulating enzyme activities (Dias et al., 2020). Regardless, our physiological results support the fact that subtropical *P. lutea* has good heat tolerance properties, mainly in terms of its resistance to bleaching and symbiotic algal retention under heat stress (Brown et al., 1999; Hoadley et al., 2021; Keshavmurthy et al., 2021).

DEGs can, to some extent, clarify the differences in resistance molecules among coral hosts (Maor-Landaw et al., 2017; Voolstra et al., 2021). Under heat stress, the DEGs of the DY coral hosts were much higher than those of XS coral hosts, and their unique DEGs were significantly enriched in pathways related to environmental information processing and cellular processes, whereas XS corals were not significantly enriched in any pathway (Fig. 4c, d). This finding indicates that the transcriptional response of subtropical corals to high temperatures is stronger and more complex, while the response of tropical corals is simpler and more rapid, which may be the main reason for the differences in phenotypes and physiology between the two groups of corals (Ip et al., 2022). In addition, temperatures triggered the DNA damage response (DDR) of DY *P. lutea* and activated the upstream factors ATM/ATR. ATM/ATR is a member of the PI3 family of serine-threonine kinases that plays a role in protecting cells from DNA damage (Maréchal and Zou, 2013). In this pathway, ATM/ATR phosphorylates CHK1 and CHK2 kinases, respectively, initiating a series of reactions that ultimately trigger the cell repair pathway. The genetic material of DY *P. lutea* hosts may be damaged, potentially due to excessive ROS production (Schwarz et al., 2012). However, DY *P. lutea* can actively participate in DNA damage repair to maintain the integrity of cell chromosomes during the process of resisting high-temperature stress, which may enhance its heat tolerance (Downs et al., 2002). However, compared to DY *P. lutea*, the DEGs of XS *P. lutea* were only enriched in pathways related to disease infection, although not significantly (Fig. 4c). This suggests that XS *P. lutea* may be susceptible to infections at extremely high temperatures. Proteasomes can degrade proteins through ubiquitination and play a key role in maintaining cellular protein homeostasis and stress responses (Basler and Groettrup, 2021). Proteasome expression in DY C15 cells may lead to the accumulation of misfolded and damaged proteins, affecting cellular protein homeostasis

(Basler and Groettrup, 2021; Pei et al., 2022). However, proteasome inhibition may indirectly activate the expression of HSP expression to enhance cellular thermotolerance and trigger the unfolded protein response to reduce misfolded protein aggregation (Schubert et al., 2000; Seveso et al., 2019). While these perspectives may appear contradictory, further research is necessary to comprehend the intricacies of coral-symbiont relationships and the associated trade-offs. Another study has reported a functional link between the ubiquitin-like (UBL) family and pre-mRNA splicing processes (Chanarat and Mishra, 2018). Thus, the co-downregulated expression of spliceosomes and proteasomes in DY C15 cells may further illustrate their relationship and their potential impact on thermotolerance. RNA polymerase is related to the transcription of genetic information of gene DNA in organisms and its expression was downregulated in XS C15 cells, indicating restricted transcription.

In general, at 34 °C, DY *P. lutea* suffered less stress and DNA oxidative damage than XS corals and could actively mediate heat stress. For XS *P. lutea*, this temperature may have exceeded its maximum tolerance temperature critical point, resulting in a higher degree of bleaching than that observed in DY *P. lutea*. Therefore, our results suggest that subtropical *P. lutea* in the SCS has a higher thermal tolerance and adaptive potential than tropical *P. lutea*. This result is also supplemented by the expansion of previous data. Previous studies have shown that the high level of genetic differentiation between subtropical DY *P. lutea* populations in the SCS and other geographical populations of *P. lutea* (Huang et al., 2018) may have enabled it to adapt to cold winter sea temperatures at the genetic level and show enhanced cold tolerance (Huang et al., 2022). This further illustrates that the wide range of phenotypic differences in thermal tolerance among corals in the SCS at different latitudes may be attributed to geographical distance and different temperature histories, benefiting from limited gene flow. This, under the synergistic effect of genetic drift and natural selection, promotes phenotypic variation and adaptation to local thermal conditions of *P. lutea* populations at different spatial scales in the SCS (Marzoni et al., 2022; Pinsky et al., 2023). Therefore, we posit that the greater heat resistance of DY *P. lutea* and its symbionts at the transcriptional level (genes related to genetic information, spliceosomes, and proteasomes) may be the result of genetic differentiation, and may have

generated inherent genetic variation during long-term natural selection.

#### 4.3. Potential temperature tolerance mechanisms in subtropical *P. lutea* in the SCS

Notably, previous studies on cold stress in tropical XS and subtropical DY *P. lutea* populations in the SCS used samples from the same batch of isolates as the experimental corals used in the present study to avoid potential individual variation and genetic background effects (Huang et al., 2022). Combined with the previous results of cold stress studies, it is evident that subtropical DY *P. lutea* in the SCS exhibits a stronger temperature tolerance and adaptability potential than tropical XS *P. lutea*. Therefore, by comparing the results of this study with those in a previous study by Huang et al. (2022) on cold stress in XS and DY *P. lutea*, we found that various transcriptional regulatory pathways participated in both cold and heat stress in DY *P. lutea* (Fig. 5 and Table S3). Continuous exposure to heat or cold can cause severe oxidative stress in coral hosts and symbionts, resulting in immune damage, damage to nucleotides and algal photosynthetic systems, and energy dissipation (Hernández Elizárraga et al., 2023). Corals and their algae activate antioxidant systems to clear excess ROS and reduce damage. Corals also change their metabolism to meet their energy distribution and supply needs for immunity and repair (Yu et al., 2023). In the process of removing active oxygen and oxygen free radicals, CAT degrades H<sub>2</sub>O<sub>2</sub> generated by O<sub>2</sub><sup>-</sup> (catalyzed by SOD), and converts it into H<sub>2</sub>O and O<sub>2</sub> (Anithajothi et al., 2014). Similarly, ROS can be removed by antioxidants, such as POD and GSH, to reduce damage to lipids and DNA (M. K. DeSalvo et al., 2008). Our results found that ROS signaling also triggers NFκB-mediated cellular inflammation, apoptosis, and innate immune responses (DeSalvo et al., 2010; Souter et al., 2011). During this process, corals alleviate ROS-induced stress ROS by regulating the signal transduction systems related to cell proliferation (such as PI3K-AKT, MAPK, and mTOR) to maintain their immune balance, which is particularly important for maintaining cell homeostasis and adapting to the environment (Ocampo et al., 2015; Voss et al., 2023). Notably, the thermotolerance transcriptional regulatory pathways discovered in this study were identical to the transcriptional responses of thermotolerant *P. lutea* to high-temperature stress in intertidal rock pools (Huang et al., 2024). Therefore, we inferred that these stress transcriptional regulatory strategies may be the common and core transcriptomes mediating *P. lutea* tolerance to higher/lower temperature stress and that these common response modes, once activated, can effectively help *P. lutea* reduce the threat posed by temperature stress. Therefore, the molecular mechanisms discovered in this study provide strong theoretical guidance for evaluating the response of tolerant reef-building corals to global climate change.

Coral reef ecosystems are severely degraded worldwide owing to global warming (Hughes et al., 2017). Identifying highly resistant coral species and introducing meaningful adaptive variation through genetic rescue or relocated selective breeding may offer a strategy to mitigate the impact of climate change on stony corals (Dixon et al., 2015; Quigley, 2023). Our results suggest that *P. lutea* in the subtropical DY of the SCS exhibits strong physiological plasticity, temperature tolerance, and adaptive potential and may have adapted to the seasonally fluctuating, wide range (14–28 °C) SST environment at the genetic level, and may be a potential candidate population to withstand future climate disturbances. Therefore, we posit that other relatively high-latitude coral populations, such as DY *P. lutea* in the subtropics of the SCS, may exhibit comparable temperature tolerance, and these corals may serve as resilient parents for sexual reproduction to promote heat-tolerant genotypes in their offspring (Bay et al., 2017; Dixon et al., 2015; Quigley et al., 2020). In particular, attention should be paid to the importance of susceptible branching corals in helping to restore coral reef communities, owing to their rapid growth and good domestication potential. This requires more work in the future to conduct similar research and verification on severely degraded branching corals to

promote coral reef recovery.

Notably, our results also highlight the importance of protecting coral reef habitats. Although some coral species (such as DY *P. lutea*) have the ability to tolerate a wide range of temperature changes (12–34 °C), climatic conditions are unfavorable for most coral species in high latitudes (Kim et al., 2019). Corals in marginal areas have limited resilience to the ongoing impacts of climate change (including exposure to harsh environments and human activities) (Hughes et al., 2003; Hughes et al., 2017). Thus, their temperature plasticity may be lost within decades without appropriate conservation and management strategies (Pandolfi et al., 2011; Pinsky et al., 2023).

## 5. Conclusion

In this study, we explored and analyzed the heat stress response of tropical XS and subtropical DY *P. lutea* populations in the SCS, and found that *P. lutea* mediates heat stress mainly by enhancing host metabolism levels to increase energy supply as a survival strategy. We also found considerable differences in heat tolerance among *P. lutea* at different latitudes in the SCS, with subtropical *P. lutea* showing greater resistance to heat stress than tropical *P. lutea*. The main manifestations are DY corals (1) have good physiological conditions under high-temperature environment, with low bleaching degree, high zooxanthellae density, *Fv/Fm* value, and chlorophyll *a* content, although XS corals have high enzyme activity; (2) live in seasonally fluctuating seawater temperatures (14–28 °C) year-round, with a wide range of temperature tolerance; and (3) have a negative-feedback transcriptional regulation strategy, namely, active environmental stress response and repair of genetic information damage. Simultaneously, combined with previous cold stress and population genetics studies, we posit *P. lutea* in the subtropical SCS has stronger temperature tolerance and adaptability potential than those in the tropical SCS, which may mediate their adaption to climate change.

## CRediT authorship contribution statement

**Wen Huang:** Writing – review & editing, Validation, Resources, Project administration, Methodology, Funding acquisition, Conceptualization. **Jinlian Chen:** Writing – original draft, Visualization, Validation, Methodology, Data curation. **Enguang Yang:** Resources, Methodology, Investigation, Data curation. **Linqing Meng:** Methodology, Data curation. **Yi Feng:** Visualization, Software. **Yinmin Chen:** Visualization, Software. **Zhihua Huang:** Validation, Methodology. **Ronghua Tan:** Validation, Methodology. **Zunyong Xiao:** Software, Formal analysis. **Yupeng Zhou:** Software, Formal analysis. **Mingpei Xu:** Software, Formal analysis. **Kefu Yu:** Writing – review & editing, Resources, Project administration, Funding acquisition, Conceptualization.

## Declaration of competing interest

The author declares no conflict of interest.

## Acknowledgements

We thank Sansha Track Ocean Coral Reef Protection Institute for collecting specimens in Xisha. We would like to thank Editage ([www.editage.cn](http://www.editage.cn)) for English language editing. This study was financially supported by the National Natural Science Foundation of China (grant nos. 42030502 and 42090041) and Guangxi Natural Science Foundation (grant nos. 2023GXNSFAA026510).

## Appendix A. Supplementary data

Supplementary data to this article can be found online at <https://doi.org/10.1016/j.scitotenv.2025.178381>.

## Data availability

The 5 km daily average sea surface temperature data for the tropical Xisha and subtropical Daya Bay areas of the South China Sea can be obtained from NOAA's Coral Reef Watch (<https://coralreefwatch.noaa.gov>). The raw read data have been deposited in the Sequence Read Archive (SRA) database at NCBI under Bioproject IDs PRJNA994659 and PRJNA810338.

## References

- Ainsworth, T.D., Heron, S.F., Ortiz, J.C., Mumby, P.J., Grech, A., Ogawa, D., Eakin, C.M., Leggat, W., 2016. Climate change disables coral bleaching protection on the Great Barrier Reef. *Science* 352, 338–342. <https://doi.org/10.1126/science.aac7125>.
- Anithajothi, R., Duraikannu, K., Umagowsalya, G., Ramakritinan, C.M., 2014. The presence of biomarker enzymes of selected scleractinian corals of Palk Bay, southeast coast of India. *Biomed. Res. Int.* 2014. <https://doi.org/10.1155/2014/684874>.
- Anthony, K.R.N., Hoogenboom, M.O., Maynard, J.A., Grottolli, A.G., Middlebrook, R., 2009. Energetics approach to predicting mortality risk from environmental stress: a case study of coral bleaching. *Funct. Ecol.* 23, 539–550. <https://doi.org/10.1111/j.1365-2435.2008.01531.x>.
- Barfield, S.J., Aglyamova, G.V., Bay, L.K., Matz, M.V., 2018. Contrasting effects of *Symbiodinium* identity on coral host transcriptional profiles across latitudes. *Mol. Ecol.* 27, 3103–3115. <https://doi.org/10.1111/mec.14774>.
- Barker, V., 2018. Exceptional thermal tolerance of coral reefs in American Samoa. *Curr. Clim. Chang. Rep.* 4, 417–427. <https://doi.org/10.1007/s40641-018-0112-3>.
- Basler, M., Groettrup, M., 2021. On the role of the immunoproteasome in protein homeostasis. *Cells* 10. <https://doi.org/10.3390/cells10113216>.
- Bay, R.A., Rose, N.H., Logan, C.A., Palumbi, S.R., 2017. Genomic models predict successful coral adaptation if future ocean warming rates are reduced. *Sci. Adv.* 3. <https://doi.org/10.1126/sciadv.1701413>.
- Bilger, W., Schreiber, U., Bock, M., 1995. Determination of the quantum efficiency of photosystem II and of non-photochemical quenching of chlorophyll fluorescence in the field. *Oecologia* 102, 425–432. <https://doi.org/10.1007/bf00341354>.
- Brown, B.E., Dunne, R.P., Ambarsari, I., Le Tissier, M.D.A., Satapoomin, U., 1999. Seasonal fluctuations in environmental factors and variations in symbiotic algae and chlorophyll pigments in four Indo-Pacific coral species. *Mar. Ecol. Prog. Ser.* 191, 53–69. <https://doi.org/10.3354/meps191053>.
- Bruno, J.F., Edmunds, P.J., 1997. Clonal variation for phenotypic plasticity in the coral *Madracis mirabilis*. *Ecology* 78, 2177–2190. [https://doi.org/10.1890/0012-9658\(1997\)078\[2177:cvfppi\]2.0.co;2](https://doi.org/10.1890/0012-9658(1997)078[2177:cvfppi]2.0.co;2).
- Buerger, P., Alvarez-Roa, C., Coppin, C.W., Pearce, S.L., Chakravarti, L.J., Oakeshoff, J. G., Edwards, O.R., van Oppen, M.J.H., 2020. Heat-evolved microalgal symbionts increase coral bleaching tolerance. *Sci. Adv.* 6. <https://doi.org/10.1126/sciadv.aba2498>.
- Chanarat, S., Mishra, S.K., 2018. Emerging roles of ubiquitin-like proteins in pre-mRNA splicing. *Trends Biochem. Sci.* 43, 896–907. <https://doi.org/10.1016/j.tibs.2018.09.001>.
- Chen, B., Yu, K., Liang, J., Huang, W., Wang, G., Su, H., Wang, Y., 2019. Latitudinal variation in the molecular diversity and community composition of symbiodiniaceae in coral from the South China Sea. *Front. Microbiol.* 10. <https://doi.org/10.3389/fmicb.2019.01278>.
- Chow, M.H., Tsang, R.H.L., Lam, E.K.Y., Ang, P., 2016. Quantifying the degree of coral bleaching using digital photogrammetric technique. *J. Exp. Mar. Biol. Ecol.* 479, 60–68. <https://doi.org/10.1016/j.jembe.2016.03.003>.
- Coleman, A.W., Suarez, A., Goff, L.J., 1994. Molecular delineation of species and syngens in volvocacean green algae (chlorophyta) 1. *J. Phycol.* 30 (1), 80–90. <https://doi.org/10.1111/j.0022-3646.1994.00080.x>.
- Coles, S.L., Riegl, B.M., 2013. Thermal tolerances of reef corals in the Gulf: a review of the potential for increasing coral survival and adaptation to climate change through assisted translocation. *Mar. Pollut. Bull.* 72 (2), 323–332. <https://doi.org/10.1016/j.marpolbul.2012.09.006>.
- D'Angelo, C., Hume, B.C., Burt, J., Smith, E.G., Achterberg, E.P., Wiedenmann, J., 2015. Local adaptation constrains the distribution potential of heat-tolerant *Symbiodinium* from the Persian/Arabian Gulf. *ISME J.* 9 (12), 2551–2560. <https://doi.org/10.1038/ismej.2015.80>.
- DeSalvo, M.K., Woolstra, C.R., Sunagawa, S., Schwarz, J.A., Stillman, J.H., Coffroth, M. A., Szmant, A.M., Medina, M., 2008. Differential gene expression during thermal stress and bleaching in the Caribbean coral *Montastraea faveolata*. *Mol. Ecol.* 17, 3952–3971. <https://doi.org/10.1111/j.1365-294x.2008.03879.x>.
- DeSalvo, M.K., Sunagawa, S., Woolstra, C.R., Medina, M., 2010. Transcriptomic responses to heat stress and bleaching in the Elkhorn coral *Acropora palmata*. *Mar. Ecol. Prog. Ser.* 402, 97–113. <https://doi.org/10.3354/meps08372>.
- Desjardins, P., Conklin, D., 2010. NanoDrop microvolume quantitation of nucleic acids. *Jove-J. Vis. Exp.* 93. <https://doi.org/10.3791/2565>.
- Dias, M., Madeira, C., Jogee, N., Ferreira, A., Gouveia, R., Cabral, H., Diniz, M., Vinagre, C., 2020. Integrative indices for health assessment in reef corals under thermal stress. *Ecol. Indic.* 113. <https://doi.org/10.1016/j.ecolind.2020.106230>.
- Dixon, G.B., Davies, S.W., Aglyamova, G.V., Meyer, E., Bay, L.K., Matz, M.V., 2015. Genomic determinants of coral heat tolerance across latitudes. *Science* 348, 1460–1462. <https://doi.org/10.1126/science.1261224>.
- Dodd, R.B., Drickamer, K., 2001. Lectin-like proteins in model organisms: implications for evolution of carbohydrate-binding activity. *Glycobiology* 11, 71R–79R. <https://doi.org/10.1093/glycob/11.5.71r>.
- Downs, C.A., Fauth, J.E., Halas, J.C., Dustan, P., Bemiss, J., Woodley, C.M., 2002. Oxidative stress and seasonal coral bleaching. *Free Radical Bio. Med.* 33, 533–543. [https://doi.org/10.1016/s0891-5849\(02\)00907-3](https://doi.org/10.1016/s0891-5849(02)00907-3).
- Evensen, N.R., Fine, M., Perna, G., Woolstra, C.R., Barshis, D.J., 2021. Remarkably high and consistent tolerance of a Red Sea coral to acute and chronic thermal stress exposures. *Limnol. Oceanogr.* 66 (5), 1718–1729. <https://doi.org/10.1002/lno.11715>.
- Hazraty-Kari, S., Morita, M., Tavakoli-Kolour, P., Nakamura, T., Harii, S., 2023. Reactions of juvenile coral to three years of consecutive thermal stress. *Sci. Total Environ.* 863, 161227. <https://doi.org/10.1016/j.scitotenv.2022.161227>.
- Hazraty-Kari, S., Tavakoli-Kolour, P., Nakamura, T., Morita, M., 2024. Susceptibility of *Acropora tenuis* to consecutive thermal stress. *Coral Reefs* 43 (4), 1097–1107. <https://doi.org/10.1007/s00338-024-02530-8>.
- Hernández Elizárraga, V.H., Olguín-López, N., Hernández-Matehuala, R., Caballero-Pérez, J., Ibarra-Alvarado, C., Rojas-Molina, A., 2023. Transcriptomic differences between bleached and unbleached hydrozoan *Millepora complanata* following the 2015–2016 ENSO in the Mexican Caribbean. *PeerJ* 11. <https://doi.org/10.7717/peerj.14626>.
- Hoadley, K.D., Pettay, D.T., Lewis, A., Wham, D., Grasso, C., Smith, R., Warner, M.E., 2021. Different functional traits among closely related algal symbionts dictate stress endurance for vital Indo-Pacific reef-building corals. *Glob. Chang. Biol.* 27 (20), 5295–5309. <https://doi.org/10.1111/gcb.15799>.
- Hoegh-Guldberg, O., 1999. Climate change, coral bleaching and the future of the world's coral reefs. *Mar. Freshw. Res.* 50, 839–866. <https://doi.org/10.1071/mf99078>.
- Howells, E.J., Abrego, D., Meyer, E., Kirk, N.L., Burt, J.A., 2016. Host adaptation and unexpected symbiont partners enable reef-building corals to tolerate extreme temperatures. *Glob. Chang. Biol.* 22, 1702–2714. <https://doi.org/10.1111/gcb.13250>.
- Huang, D., Licuanan, W.Y., Hoeksema, B.W., Chen, C.A., Ang, P.O., Huang, H., Chou, L. M., 2015. Extraordinary diversity of reef corals in the South China Sea. *Mar. Biodivers.* 45, 157–168. <https://doi.org/10.1007/s12526-014-0236-1>.
- Huang, H., Zhang, C.L., Yang, J.H., You, F., Lian, J.S., Tan, Y.H., 2012. Scleractinian coral community characteristics in Zhuhai reef sea area of Nansha Islands. *J. Oceanogr. Taiwan St* 31, 79–84. <https://doi.org/10.3969/j.issn.1000-8160.2012.01.012>.
- Huang, W., Li, M., Yu, K., Wang, Y., Li, J., Liang, J., Wei, F., 2018. Genetic diversity and large-scale connectivity of the scleractinian coral *Porites lutea* in the South China Sea. *Coral Reefs* 37, 1259–1271. <https://doi.org/10.1007/s00338-018-1724-8>.
- Huang, W., Yang, E., Yu, K., Meng, L., Wang, Y., Liang, J., Huang, X., Wang, G., 2022. Lower cold tolerance of tropical *Porites lutea* is possibly detrimental to its migration to relatively high latitude refuges in the South China Sea. *Mol. Ecol.* 31, 5339–5355. <https://doi.org/10.1111/mec.16662>.
- Huang, W., Meng, L., Xiao, Z., Tan, R., Yang, E., Wang, Y., Huang, X., Yu, K., 2024. Heat-tolerant intertidal rock pool coral *Porites lutea* can potentially adapt to future warming. *Mol. Ecol.* 33. <https://doi.org/10.1111/mec.12723>.
- Hughes, T.P., Barnes, M.L., Bellwood, D.R., Cinner, J.E., Cumming, G.S., Jackson, J.B., Scheffer, M., 2017. Coral reefs in the Anthropocene. *Nature* 546 (7656), 82–90. <https://doi.org/10.1038/nature22901>.
- HughesTP, B., BellwoodDR, C., ConnollySR, F., GrosbergR, H.G., JacksonJB, K., Lough, J. M., RosenB, R., 2003. Climate change, human impacts, and the resilience of coral reefs. *Science* 301, 929–933. <https://doi.org/10.1126/science.1085046>.
- Ip, J.C.-H., Zhang, Y., Xie, J.Y., Yeung, Y.H., Qiu, J.-W., 2022. Comparative transcriptomics of two coral holobionts collected during the 2017 El Niño heat wave reveal differential stress response mechanisms. *Mar. Pollut. Bull.* 411, 41–42. <https://doi.org/10.1016/j.marpolbul.2022.114017>.
- Jeffrey, S.T., Humphrey, G.F., 1975. New spectrophotometric equations for determining chlorophylls a, b, c1 and c2 in higher plants, algae and natural phytoplankton. *Biochem. Physiol. Pflanzen* 167 (2), 191–194. [https://doi.org/10.1016/S0015-3796\(17\)30778-3](https://doi.org/10.1016/S0015-3796(17)30778-3).
- Jeong, H., Mason, S.P., Barabási, A.L., Oltvai, Z.N., 2001. Lethality and centrality in protein networks. *Nature* 411, 41–42. <https://doi.org/10.1038/35075138>.
- Johannes, R.E., Coles, S.L., Kuenzel, N.T., 1970. The role of zooplankton in the nutrition of some Scleractinian corals 1. *Limnol. Oceanogr.* 15 (4), 579–586. <https://doi.org/10.4319/lo.1970.15.4.0579>.
- Keshavmurthy, S., Beals, M., Hsieh, H.J., Choi, K.S., Chen, C.A., 2021. Physiological plasticity of corals to temperature stress in marginal coral communities. *Sci. Total Environ.* 758, 143628. <https://doi.org/10.1016/j.scitotenv.2020.143628>.
- Kim, D., Perteza, G., Trapnell, C., Pimentel, H., Kelley, R., Salzberg, S.L., 2013. TopHat2: accurate alignment of transcriptomes in the presence of insertions, deletions and gene fusions. *Genome Biol.* 14. <https://doi.org/10.1186/gb-2013-14-4-r36>.
- Kim, S.W., Sampayo, E.M., Sommer, B., Sims, C.A., Gómez-Cabrera, M.D.C., Dalton, S.J., Pandolfi, J.M., 2019. Refugia under threat: mass bleaching of coral assemblages in high-latitude eastern Australia. *Glob. Chang. Biol.* 25, 3918–3931. <https://doi.org/10.1111/gcb.14772>.
- Lajeunesse, T.C., Trench, R.K., 2000. Biogeography of two species of *Symbiodinium* (Freudenthal) inhabiting the intertidal sea anemone *Anthopleura elegantissima* (Brandt). *Biol. Bull.* 199, 126–134. <https://doi.org/10.2307/1542872>.
- Langlais, C.E., Lenton, A., Heron, S.F., Evenhuis, C., Sen Gupta, A., Brown, J.N., Kuchinke, M., 2017. Coral bleaching pathways under the control of regional temperature variability. *Nat. Clim. Chang.* 7 (7(11)), 839–844. <https://doi.org/10.1038/nclimate3399>.
- Lenth, R., Singmann, H., Love, J., Buerkner, P., Herve, M., 2019. emmeans: estimated marginal means, aka least-squares means. R package version 1.4.5. <https://cran.r-project.org/web/packages/emmeans/index.html>.



- Li, B., Dewey, C.N., 2011. RSEM: accurate transcript quantification from RNA-Seq data with or without a reference genome. *BMC Bioinform.* 12. <https://doi.org/10.1186/1471-2105-12-323>.
- Li, J., Chen, Q., Zhang, S., Huang, H., Yang, J., Tian, X.-P., Long, L.-J., 2013. Highly heterogeneous bacterial communities associated with the South China Sea reef corals *Porites lutea*, *Galaxea fascicularis* and *Acropora millepora*. *PloS One* 8. <https://doi.org/10.1371/journal.pone.0071301>.
- Love, M.I., Huber, W., Anders, S., 2014. Moderated estimation of fold change and dispersion for RNA-seq data with DESeq2. *Genome Biol.* 15. <https://doi.org/10.1186/s13059-014-0550-8>.
- Luo, Y., Huang, W., Yu, K., Li, M., Chen, B., Huang, X., Qin, Z., 2022. Genetic diversity and structure of tropical *Porites lutea* populations highlight their high adaptive potential to environmental changes in the South China Sea. *Front. Mar. Sci.* 9. <https://doi.org/10.3389/fmars.2022.791149>.
- Manzello, D.P., Matz, M.V., Enochs, I.C., Valentino, L., Carlton, R.D., Kolodziej, G., Jankulak, M., 2019. Role of host genetics and heat-tolerant algal symbionts in sustaining populations of the endangered coral *Orbicella faveolata* in the Florida Keys with ocean warming. *Glob. Chang. Biol.* 25, 1016–1031. <https://doi.org/10.1111/gcb.14545>.
- Maor-Landaw, K., et al., 2017. Mediterranean versus Red Sea corals facing climate change, a transcriptome analysis. *Sci. Rep.* 7. <https://doi.org/10.1038/srep42405>.
- Maréchal, A., Zou, L., 2013. DNA damage sensing by the ATM and ATR kinases. *Csh. Perspect. Biol.* 5. <https://doi.org/10.1101/cshperspect.a012716>.
- Marzonic, M.R., Bay, L.K., Bourne, D.G., Hoey, A.S., Matthews, S., Nielsen, J.J.V., Harrison, H.B., 2022. The effects of marine heatwaves on acute heat tolerance in corals. *Glob. Chang. Biol.* 29, 404–416. <https://doi.org/10.1111/gcb.16473>.
- Masoudi, M., Asrari, E., 2023. Hazard assessment of global warming around the world using GIS. *Environ. Monit. Assess.* 195 (9), 1025. <https://doi.org/10.1007/s10661-023-11464-7>.
- Mumby, Peter J., van Woesik, R., 2014. Consequences of ecological, evolutionary and biogeochemical uncertainty for coral reef responses to climatic stress. *Curr. Biol.* 24, R413–R423. <https://doi.org/10.1016/j.cub.2014.04.029>.
- Ocampo, I.D., Zárate-Potes, A., Pizarro, V., Rojas, C.A., Vera, N.E., Cadavid, L.F., 2015. The immunotranscriptome of the Caribbean reef-building coral *Pseudodiploria strigosa*. *Immunogenetics* 67, 515–530. <https://doi.org/10.1007/s00251-015-0854-1>.
- Osman, E.O., Smith, D.J., Ziegler, M., Kürten, B., Conrad, C., El-Haddad, K.M., Woolstra, C.R., Suggett, D.J., 2017. Thermal refugia against coral bleaching throughout the northern Red Sea. *Glob. Chang. Biol.* 24. <https://doi.org/10.1111/gcb.13895>.
- Palumbi, S.R., Barshis, D.J., Traylor-Knowles, N., Bay, R.A., 2014. Mechanisms of reef coral resistance to future climate change. *Science* 344 (6186), 895–898. <https://doi.org/10.1126/science.1251336>.
- Pandolfi, J.M., Connolly, S.R., Marshall, D.J., Cohen, A.L., 2011. Projecting coral reef futures under global warming and ocean acidification. *Science* 333, 418–422. <https://doi.org/10.1126/science.1204794>.
- Pei, Y., Chen, S., Diao, X., Wang, X., Zhou, H., Li, Y., Li, Z., 2022. Deciphering the disturbance mechanism of BaP on the symbiosis of *Montipora digitata* via 4D-proteomics approach. *Chemosphere* 312. <https://doi.org/10.1016/j.chemosphere.2022.137223>.
- Pinsky, M.L., Clark, R.D., Bos, J.T., 2023. Coral reef population genomics in an age of global change. *Annu. Rev. Genet.* 57, 87–115. <https://doi.org/10.1146/annurev-genet-022123-102748>.
- Qin, Z., Yu, K., Chen, B., Wang, Y., Liang, J., Luo, W., Xu, L., Huang, X., 2019. Diversity of Symbiodiniaceae in 15 coral species from the Southern South China Sea: potential relationship with coral thermal adaptability. *Front. Microbiol.* 10. <https://doi.org/10.3389/fmicb.2019.02343>.
- Quigley, K.M., 2023. Breeding and selecting corals resilient to global warming. *Annu. Rev. Anim. Biosci.* 12, 209–232. <https://doi.org/10.1146/annurev-animal-021122-093315>.
- Quigley, K.M., Bay, L.K., van Oppen, M.J.H., 2020. Genome-wide SNP analysis reveals an increase in adaptive genetic variation through selective breeding of coral. *Mol. Ecol.* 29, 2176–2188. <https://doi.org/10.1111/mec.15482>.
- Robbins, S.J., Singleton, C.M., Chan, C.X., Messer, L.F., Geers, A.U., Ying, H., Bourne, D.G., 2019. A genomic view of the reef-building coral *Porites lutea* and its microbial symbionts. *Nat. Microbiol.* 4, 2090–2100. <https://doi.org/10.1038/s41564-019-0532-4>.
- Rowan, H.M., James, T.P., Agustí, M.-G., Noah, L.W., Christopher, P.J., Robert, J.T., Andréa, G.G., 2021. Environmental gradients drive physiological variation in Hawaiian corals. *Coral Reefs* 40, 1505–1523. <https://doi.org/10.1007/s00338-021-02140-8>.
- Savary, R., Barshis, D.J., Woolstra, C.R., Cárdenas, A., Evensen, N.R., Banc-Prandi, G., Fine, M., Meibom, A., 2021. Fast and pervasive transcriptomic resilience and acclimation of extremely heat-tolerant coral holobionts from the northern Red Sea. *Proc. Natl. Acad. Sci.* 118. <https://doi.org/10.1073/pnas.2023298118>.
- Schubert, U., Antón, L.C., Gibbs, J., Norbury, C.C., Yewdell, J.W., Bennink, J.R., 2000. Rapid degradation of a large fraction of newly synthesized proteins by proteasomes. *Nature* 404, 770–774. <https://doi.org/10.1038/35008096>.
- Schwarz, J.A., Mitchelmore, C.L., Jones, R., O’Dea, A., Seymour, S., 2012. Exposure to copper induces oxidative and stress responses and DNA damage in the coral *Montastraea franksi*. *Comp. Biochem. Phys. C* 157, 272–279. <https://doi.org/10.1016/j.cbpc.2012.12.003>.
- Selmoni, O., Bay, L.K., Exposito-Alonso, M., Cleves, P.A., 2024. Finding genes and pathways that underlie coral adaptation. *Trends Genet.* 40, 213–227. <https://doi.org/10.1016/j.tig.2024.01.003>.
- Seveso, D., Arrigoni, R., Montano, S., Maggioni, D., Orlandi, I., Berumen, M.L., Galli, P., Vai, M., 2019. Investigating the heat shock protein response involved in coral bleaching across scleractinian species in the central Red Sea. *Coral Reefs* 39, 85–98. <https://doi.org/10.1007/s00338-019-01878-6>.
- Souter, P., Bay, L., Andreakis, N., Csaszar, N., Seneca, F., Van Oppen, M., 2011. A multilocus, temperature stress-related gene expression profile assay in *Acropora millepora*, a dominant reef-building coral. *Mol. Ecol. Resour.* 11 (2), 328–334. <https://doi.org/10.1111/j.1755-0998.2010.02923.x>.
- Sully, S., Burkepile, D.E., Donovan, M.K., Hodgson, G., van Woesik, R., 2019. A global analysis of coral bleaching over the past two decades. *Nat. Commun.* 10. <https://doi.org/10.1038/s41467-019-09238-2>.
- Tavakoli-Kolour, P., Sinniger, F., Morita, M., Nakamura, T., Harii, S., 2023. Variability in thermal stress thresholds of corals across depths. *Front. Mar. Sci.* 10, 1210662. <https://doi.org/10.3389/fmars.2023.1210662>.
- Woolstra, C.R., Buitrago-Lopez, C., Perna, G., Cardenas, A., Hume, B.C.C., Raedecker, N., Barshis, D.J., 2020. Standardized short-term acute heat stress assays resolve historical differences in coral thermotolerance across microhabitat reef sites. *Glob. Chang. Biol.* 26 (8), 4328–4343. <https://doi.org/10.1111/gcb.15148>.
- Woolstra, C.R., Valenzuela, J.J., Turkarslan, S., Cárdenas, A., Hume, B.C., Perna, G., Barshis, D.J., 2021. Contrasting heat stress response patterns of coral holobionts across the Red Sea suggest distinct mechanisms of thermal tolerance. *Mol. Ecol.* 30, 4466–4480. <https://doi.org/10.1111/mec.16064>.
- Voss, P.A., Gornik, S.G., Jacobovitz, M.R., Rupp, S., Dörr, M., Maegele, I., Guse, A., 2023. Host nutrient sensing is mediated by mTOR signaling in cnidarian-dinoflagellate symbiosis. *Curr. Biol.* 33. <https://doi.org/10.1016/j.cub.2023.07.038>.
- Warner, M.E., Fitt, W.K., Schmidt, G.W., 1999. Damage to photosystem II in symbiotic dinoflagellates: a determinant of coral bleaching. *Proc. Natl. Acad. Sci.* 98, 8007–8012. <https://doi.org/10.1073/pnas.96.14.8007>.
- Yu, K., 2012. Coral reefs in the South China Sea: their response to and records on past environmental changes. *Sci. China Earth Sci.* 55, 1217–1229. <https://doi.org/10.1007/s11430-012-4449-5>.
- Yu, X., Yu, K., Liao, Z., Chen, B., Qin, Z., Liang, J., Gao, X., 2023. Adaptation strategies of relatively high-latitude marginal reef corals in response to severe temperature fluctuations. *Sci. Total Environ.* 903. <https://doi.org/10.1016/j.scitotenv.2023.166439>.